SSRG International Journal of Electronics and Communication Engineering
ISSN: 2348-8549/ https://doi.org/10.14445/23488549/IJECE-V13I1P119

Volume 13 Issue 1, 264-274, January 2026

Original Article

A Novel ANN-Based Spectrum Sensing Framework Using Energy and Statistical Features in Cognitive Radio Networks

Manshi Shah[1], Paresh Dholakia[2]

[1]*GTU Scholar, Gujarat Technological University, India.*
[2]*VVP Engineering College, Rajkot, India.*

[1]*Corresponding Author : paresh.dholakia.ec@vvpedulink.ac.in*

Received: 10 November 2025 Revised: 12 December 2025 Accepted: 11 January 2026 Published: 14 January 2026

Abstract - *Spectrum sensing is essential in cognitive radio networks to enable dynamic spectrum access and efficient utilization of spectrum resources. Conventional methods such as energy detection, matched filter-based detection, or cyclostationary-based tests approaches have limited accuracy under AWGN and Rayleigh fading, particularly at low SNR. GoF-based and hybrid schemes provide only modest gains in challenging conditions. To address this gap, an ANN-based sensing model using four features from energy and Zhang statistics of current and previous sensing windows is proposed. Experiments with an FM dataset (94.300, 96.700, and 98.300 MHz, bandwidth 0.2 MHz) acquired at 45 dB gain and a decimation rate of 64 demonstrate its effectiveness. The model achieved 86.8% accuracy and a detection probability of 0.75 at −10 dB, reaching 1.00 at +4 dB, confirming its robustness for dynamic spectrum access.*

Keywords - *Artificial Neural Network, Cognitive Radio, Energy Detection, Rayleigh fading, Spectrum sensing.*

1. Introduction

Spectrum sensing is a core function in Cognitive Radio Networks (CRNs) because it allows secondary users to identify temporarily unused spectrum and access it while protecting licensed primary users from harmful interference [1]. With wireless traffic continuing to grow, many frequency bands experience persistent congestion, and static allocation alone cannot meet demand. Dynamic Spectrum Access (DSA), therefore, becomes a practical requirement for improving spectrum utilization and easing perceived scarcity. However, dependable sensing is still difficult in realistic settings, particularly when the received signal is weak, the Signal-to-Noise Ratio (SNR) is low, or the channel exhibits fading [2].

Although spectrum sensing has been studied for years, many established techniques struggle when the environment changes rapidly. Energy Detection (ED) is widely used because it is straightforward and computationally light, yet its reliability drops sharply in low-SNR conditions and in the presence of fading. Other classical approaches, including matched filter-based detection, cyclostationary-based detection, or Goodness-of-Fit (GoF) based tests, also have practical constraints. Matched filtering depends on accurate prior knowledge of the primary signal, while statistical tests often show inconsistent behaviour across different channel and noise conditions [3]. Some of the non-parametric GoF (Goodness-of-Fit)-based sensing schemes like Anderson–Darling, Ordered Statistics, Kolmogorov, Smirnov, and LRS-G^2 (Likelihood Ratio Statistics) have yielded better detection performance in low-SNR conditions, but still have the overall sensing ability limited.

A key weakness of ED-based methods is their dependence on energy-only evidence. Under Rayleigh fading, the energy distribution becomes highly variable, and the decision boundary becomes unstable when noise dominates. Statistical refinements such as Zhang-type measures have been introduced to strengthen detection, but when used alone, they still provide limited resilience under challenging propagation scenarios [4]. Hybrid strategies that combine ED with GoF-related indicators can improve performance to some extent, yet they typically rely on handcrafted features and do not adapt gracefully when signal characteristics drift over time.

To address these issues, this work develops an Artificial Neural Network (ANN) model for spectrum sensing that learns a decision rule directly from complementary evidence sources. The ANN takes four inputs: the energy and Zhang statistic values computed from the current sensing window and the immediately preceding window. By incorporating

short-term temporal context, the model can capture local consistency patterns that are difficult to express using fixed thresholds. Training and evaluation are conducted using real FM radio recordings centered at 94.300, 96.700, and 98.300~MHz, each with a bandwidth of 0.2~MHz. The goal is to improve detection under both AWGN and Rayleigh fading channels while avoiding the need for explicit channel knowledge.

The contributions of this study are summarized below.

- An ANN-based sensing formulation that jointly exploits energy and Zhang statistic features from consecutive sensing windows.
- Experimental validation under AWGN and Rayleigh fading using real FM radio measurements.
- A detailed analysis of how sensing block size affects detection behaviour, supported by Receiver Operating Characteristic (ROC) results.
- A discussion of practical considerations and extensions, including compact network designs and semi-supervised learning options.

The remainder of the paper is organized as follows—Section 2 reviews related spectrum sensing research. Section 3 presents the dataset, the feature computation procedure, and the proposed ANN-based method. Section 4 reports the experimental findings, and Section 5 interprets the results. Section 6 concludes the paper and outlines directions for further work.

2. Related Work

Recent works have explored diverse ML techniques for enhancing spectrum sensing in CRNs. Aygu'l et al. [5] surveyed ML-based spectrum occupancy prediction, emphasizing deep learning for correlation capture but lacking real deployment cases. Enyenihi [6] proposed an MDP–FCFS contention framework improving efficiency yet requiring heavy parameter tuning. Ahmed et al. [7] introduced a Naive Bayes energy detector avoiding threshold calculation, though tested only on AWGN channels. Sairam and Egala [8] applied adaptive thresholding to reduce errors, but it depended on precise SNR estimation.

Sekar et al. [9] developed an SVM-ENR-RBF model achieving high accuracy with increased complexity on large datasets. Chaudhary et al. [10] reviewed ML sensing approaches, noting accuracy gains but computational issues. Samala and Singh [11] combined K-means with eigenvalue-based cooperative sensing in $\alpha - \kappa - \mu$ fading channels, achieving improved ROC metrics at high computational cost. Mahmoud et al. [12] applied ML classifiers for IoMT applications, reducing false alarms by 20% but without generalization. Kumar [13] optimized spectrum sensing using ML for threshold reduction and low SNR detection, though real-data validation was absent. Wang et al. [14] proposed a CNN-LSTM collaborative sensing system with low error, but complexity-limited use on resource-constrained devices. Abdelbaset et al. [15] introduced CNN-based sensing that outperformed conventional methods in AWGN, but fading cases were not detailed. Talib et al. [16] showed LSTM reduced false alarms over energy detection, with a higher training cost. Himmawan et al. [17] applied SVM for cooperative sensing under fading, though only small-scale tests. Murti et al. [18] combined SVM and energy detection with 80% accuracy at 10 dB SNR, but performance degraded at low SNR. Venkatapathi et al. [19] improved cooperative sensing with ML but faced dynamic threshold challenges. Srinu et al. [20] propose a PINN-based sensing approach that maintains high detection at low SNR, reporting P_d above 0.90 near -12 dB with fewer samples. Its practicality is limited by the need for a clean reference signal and the added computational burden. Cifuentes et al. [21] use machine learning to mitigate SSDF attacks in cooperative sensing and report roughly 20% improvement in the evaluated setting. The main weakness is that results are demonstrated only in simulation, leaving real RF uncertainty untested. Gupta et al. [22] target CRSN longevity under PUEA by incorporating attack-aware operation, showing improved network lifetime. However, the study lacks hardware-level validation, so deployment cost and stability remain unclear. Dhaigude and Patil [23] combine LSTM prediction with optimization for better channel allocation under time-varying occupancy. Yet sensing reliability is hard to judge because P_d and P_{fa} are not reported. Emmanuel et al. [24] adopt ANFIS to adapt sensing thresholds under dynamic noise, supporting more stable decisions than fixed thresholds. The evidence is limited by small-scale simulations and uncertain generalization to real measurements.

Despite advances, robust detection under real-world conditions remains challenging. Many methods are constrained by AWGN-only testing, limited fading evaluation, or heavy parameter tuning. CNN-LSTM and hybrid ML improve accuracy but add computational cost. Power-only or statistical-only methods also fail in dynamic noise and fading. To address this, we propose an ANN-based sensing model combining energy and Zhang statistic features from current and previous windows, capturing temporal and statistical dependencies to improve accuracy and robustness in AWGN and Rayleigh fading, while remaining lightweight for cognitive radios.

3. Materials and Methods

This section presents the methodology for designing an ANN-based spectrum sensing strategy. The framework exploits energy and Zhang statistic features from current and past sensing windows to improve detection under AWGN and Rayleigh fading channels. The process includes signal modelling, feature extraction, ANN classification, and final decision making. An overview of the system architecture is shown in Figure 1.

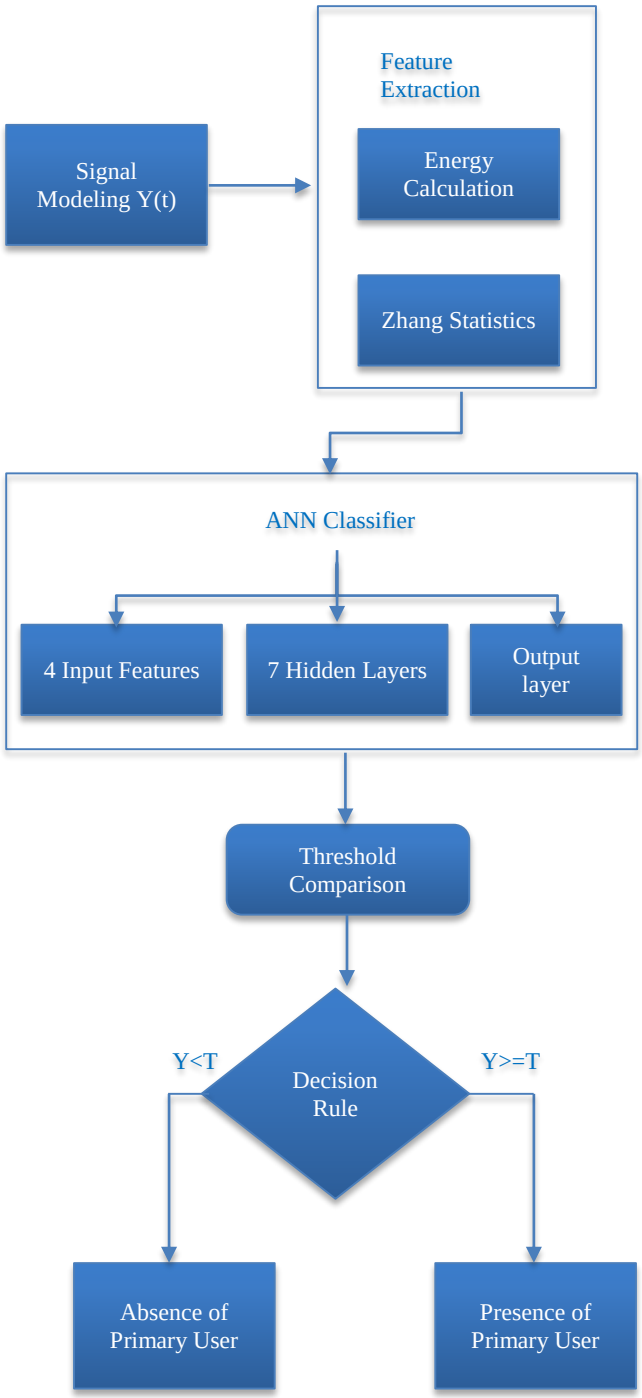

Fig. 1 Suggested ANN-based spectrum sensing model

3.1. Signal Model

In CRN, spectrum sensing is often represented in terms of a binary hypothesis test for the received signal r(t) of the secondary user. The signal representation from Equation 1 is represented by:

$$y(t) = \begin{cases} e(t), & H_0\ (no\ primary\ user\ activity) \\ m(t) + e(t), & H_1\ (primary\ user\ active) \end{cases} \quad (1)$$

In spectrum sensing, H_0 denotes an idle channel, and H_1 represents occupancy by a primary user. The received signal $y(t)$ consists of the Primary Transmission $m(t)$ and Additive White Gaussian Noise $e(t)$ with zero mean and variance σ^2. Detection becomes more challenging under impairments such as path loss, shadowing, and Rayleigh fading. The key objective is to maximize the probability of detection, $P_{d,}$ while keeping the false alarm probability, $P_{fa,}$ within acceptable limits.

3.2. Feature Extraction

The model takes 4 features, which are energy and the Zhang statistic value of the present window and the previous window. The energy statistic E, defined in Equation 2, measures received signal power:

$$E = \sum_{i=1}^{N} y_i^2 \quad (2)$$

Where y_i is the i-th sample in a window of length N. While E is sensitive to signal presence, it degrades in low SNR or fading.

Along with energy, we use the Zhang statistic as a complementary feature because it captures distribution-level deviations that energy alone can miss. Under H_0 (noise-only), the samples follow a known noise distribution, so the empirical cumulative distribution of the observed samples should align with the corresponding theoretical CDF. The Zhang statistic quantifies the mismatch between these two distributions by aggregating squared log-deviations across ordered samples, as given in (3):

$$Z_c = \sum_{i=1}^{N} \left[log \left(\frac{F_0(Y_i)^{-1} - 1}{\frac{N - \frac{1}{2}}{i - \frac{3}{4}} - 1} \right) \right]^2 \quad (3)$$

Where $F_0(y_i)$ denotes the CDF of y_i under H_0. In practice, this statistic is sensitive to structural changes in the sample distribution caused by a primary signal, which makes it useful when fading and low SNR obscure energy separation.

3.3. ANN Classifier

The Artificial Neural Network (ANN) processes the feature vector.

$$x = [E, E_P, Z_c, Z_P] \quad (4)$$

Where E and E_P Denote the energies of the current and previous sensing windows, and Z_c and Z_P Represent the Zhang statistics.

The hidden representation is obtained through the ReLU activation,

$$z = max(0, Au + \beta), \quad (5)$$

Where A and β are the weight matrix and bias. This non-linear mapping enhances feature discrimination under fading conditions.

The output probability is computed using the sigmoid function,

$$\hat{O} = \frac{1}{1+e^{-(Cz+\delta)}} \quad (6)$$

Which maps predictions between 0 and 1, interpreted as the likelihood of primary user presence. Training employs binary cross-entropy loss, and a threshold of $\theta = 0.5$ is applied for the final decision on spectrum occupancy.

3.4. Detection Performance in Rayleigh Fading Channels

In Rayleigh fading, the instant SNR γ has the exponential PDF below:

$$f_n(\eta) = \frac{1}{\eta}\exp\left(-\frac{\eta}{\bar{\eta}}\right) \quad (7)$$

Where $\bar{\eta}$ is the average SNR.

The detection probability P_d It is then calculated as the expectation over η, shown below in Equation 8:

$$P_d = \int_0^\infty Q\left(\frac{\theta - L(1+\eta)}{\sqrt{2L(1+2\eta)}}\right) f_\eta(\eta) d_\eta \quad (8)$$

Where $Q(\cdot)$ is the Gaussian Q-function, θ is the detection threshold, and L is the sensing window length. Equation 8 captures the impact of fading by integrating the conditional detection probability weighted by the SNR distribution.

Rayleigh fading introduces significant challenges to reliable detection due to the severe random attenuation of the signal, particularly at low average SNR values. $\bar{\gamma}$. As represented in Equations 7 and 8, the detection performance is strongly influenced by these channel fluctuations.

3.5. Performance Metrics

The model performance is evaluated using standard metrics for spectrum sensing. Accuracy reflects the proportion of correctly classified outcomes, while the Probability of Detection (P_d) measures the ability to identify primary user activity. The false alarm probability, P_{fa}It quantifies how often an idle channel is reported as occupied. A sensing strategy is considered dependable when it achieves a high detection probability, P_d, while keeping P_{fa} Low. This balance is most informative at low signal-to-noise ratios and under fading, where uncertainty in the received signal is greatest. In such conditions, a detector that sustains large P_d with restrained P_{fa} Provides timely and accurate spectrum availability estimates, which support stable cognitive radio operation and efficient spectrum reuse.

4. Results and Discussion

This section describes the experimental findings of the ANN-based spectrum sensing model and compares the results with conventional techniques.

Table 1. FM radio dataset parameters used for spectrum sensing

Fstart (MHz)	Fcenter (MHz)	Fstop (MHz)	Signal BW (MHz)	Gain (dB)	Decimation Rate (M)	Sampled Bandwidth (MHz)
94.100	94.300	94.500	0.2	45	64	1
96.500	96.700	96.900	0.2	45	64	1
98.100	98.300	98.500	0.2	45	64	1

Table 2. ANN configuration for the proposed model

Parameter	Value
Input Features	Energy (curr. + prev.), Zhang stat. (curr. + prev.)
Hidden Layers	1
Neurons in Hidden Layer	7
Activation (Hidden / Output)	ReLU / Sigmoid
Loss Function	Binary Cross-Entropy
Optimizer	Adam
Batch Size	250
Epochs	350
SNR Range (dB)	-20 to +4

4.1. FM Radio Dataset Parameters

The FM dataset for spectrum sensing contains three carriers centered at 94.300, 96.700, and 98.300 MHz, each with a bandwidth of 0.2 MHz (Table 1). Signals were recorded with a receiver gain of 45 dB. A decimation factor of 64 reduced the effective sampled bandwidth to 1 MHz while preserving the relevant passband characteristics. With these settings, the data retain the spectral structure of broadcast FM and provide a consistent basis for feature extraction and for evaluating the performance of the ANN-based sensing model.

4.2. ANN Configuration for Proposed Model

The configuration of the proposed network is summarized in Table 2. The input comprises four features, which pair energy and Zhang statistic values from the current and immediately preceding detections. This choice captures short-range dynamics in signal power and distributional shape. The architecture contains a single hidden layer with seven units, selected by cross-validation to control model capacity while maintaining predictive accuracy. A rectified linear unit is used in the hidden layer, and a logistic function at the output supports binary decisions. Training minimizes the binary cross-entropy objective with the Adam optimizer, using a batch size of 250 for 350 epochs. The dataset spans an SNR sweep from −20 to +4dB and includes both AWGN and Rayleigh fading, which exposes the classifier to adverse conditions and improves its reliability across channels.

4.3. Accuracy Measurement of ANN with Different Features

Table 3 compares the ANN's accuracy across feature sets and illustrates how feature choice affects spectrum sensing. Using only energy from the current and previous sensing events reaches 76.66%, which is not adequate for separating occupied and vacant states. Relying solely on the Zhang statistic increases accuracy to 83.82% by capturing the distributional structure that energy does not encode. Combining energy and Zhang from the current event yields 84.15%. The best result, 86.82%, is obtained when all four inputs—current and previous energy and Zhang values—are provided. Together, these findings show that pairing temporal context with statistical descriptors improves the classifier's decisions under challenging conditions.

Table 3. Performance accuracy of ANN with varying feature sets

Radio Technology	Only E Value (2 Features)	Only Zhang Statistic	Energy and Zhang Statistic Both	All Four Features (Proposed)
FM	76.66 %	83.82 %	84.15 %	86.82 %

Table 4. Detection probability (P_d) comparison of ANN (2 vs 4 Features) and conventional method (N = 100)

SNR (dB)	ANN (2 Features)	ANN (4 Features)	Conventional Method
-20	0.10	0.10	0.09
-18	0.13	0.15	0.09
-16	0.14	0.22	0.11
-14	0.19	0.40	0.14
-12	0.26	0.59	0.18
-10	0.37	0.75	0.26
-8	0.56	0.86	0.38
-6	0.78	0.89	0.60
-4	0.91	0.91	0.84
-2	0.94	0.95	0.98
0	0.96	0.97	0.99
+2	0.98	0.99	0.99
+4	0.99	0.99	0.99

4.4. Detection Probability of ANN Compared to Conventional Techniques

Table 4 summarizes the detection probability at representative SNR values. At −20 dB, both ANN configurations slightly exceed the conventional detector. The benefit of using four features is most visible at intermediate SNR. At −14 dB, the four-feature ANN attains Pd=0.40P_d = 0.40Pd=0.40, compared with 0.19 for the two-feature model and 0.14 for the conventional method. At −10 dB, the four-feature ANN reaches 0.75, which is markedly higher than the alternatives at the same operating point. As SNR improves, all methods converge, but the ANN consistently reaches A higher detection probability more rapidly, highlighting its robustness in low SNR conditions. Figure 2 illustrates these trends.

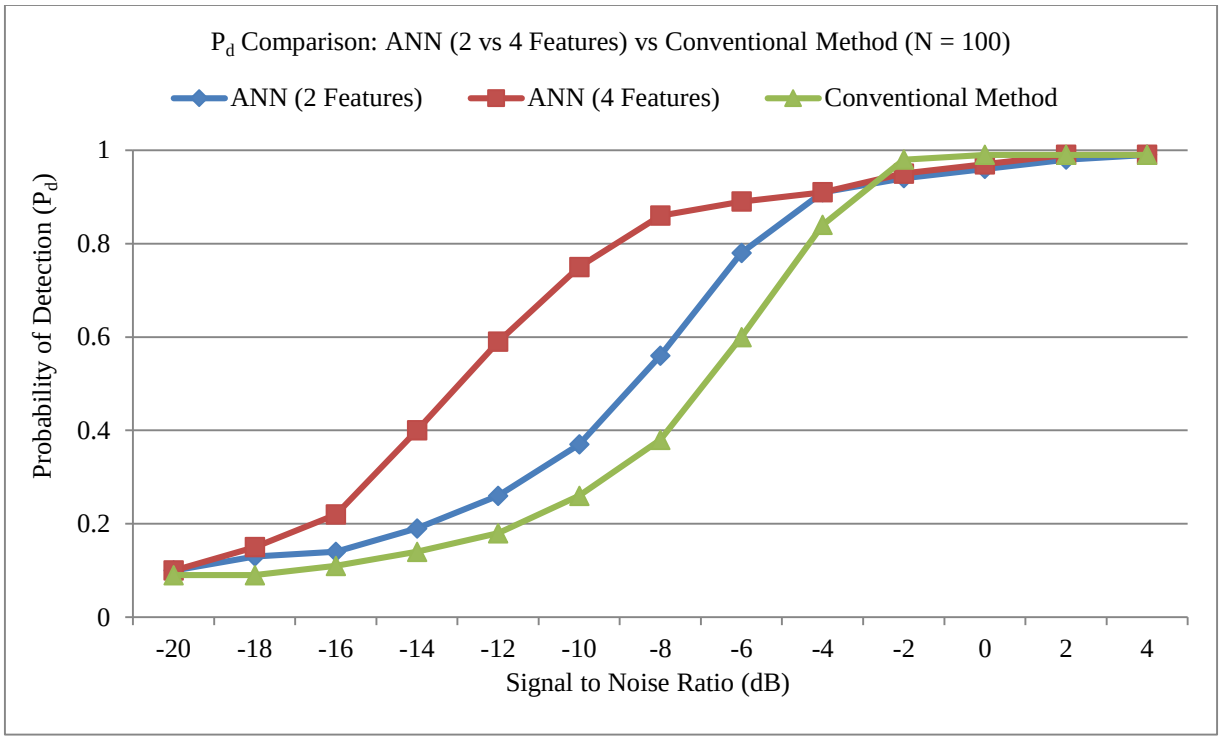

Fig. 2 Comparison of P_d vs. SNR for ANN (2 and 4 features) and the conventional method

Table 5. Classification accuracy of the ANN under AWGN and Rayleigh channels for different feature inputs

Radio Technology	Only E (AWGN)	Only E (Rayleigh)	Energy + Zhang (AWGN)	Energy + Zhang (Rayleigh)
FM	86.66 %	85.53 %	89.53 %	88.50 %

4.5. Accuracy Performance of ANN in AWGN and Rayleigh Channels

Table 5 reports the classification accuracy of the ANN under AWGN and Rayleigh channels for different feature inputs. With only energy-based features, the model attains about 86.7% accuracy in AWGN and 85.5% in Rayleigh fading, showing that it can learn effectively even under channel impairments. When both energy and Zhang statistics are included, accuracy improves to 89.5% in AWGN and 88.5% in Rayleigh. The results demonstrate that statistical features complement energy information, leading to more reliable detection. While AWGN performance remains slightly higher due to stable channel conditions, the consistent gains in Rayleigh confirm the robustness of the proposed approach for cognitive radio applications.

4.6. Detection Probability of ANN under AWGN and Rayleigh Channels Compared with Conventional ED

Table 6 and Figure 3 report detection probability for the ANN and for conventional energy detection at representative SNR values. At −20 dB, the ANN shows a small gain over energy detection in both AWGN and Rayleigh channels. The margin widens at mid-range SNR. At −10 dB, the ANN attains (P_d =0.90) in AWGN and (P_d =0.88) in Rayleigh, while energy detection remains at 0.40.

Table 6. Detection probability (P_d) comparison of ANN and conventional ED under AWGN and rayleigh channels

SNR (dB)	AWGN (ANN)	Rayleigh Fading (ANN)	Conventional ED Simulation
-20	0.18	0.14	0.13
-18	0.26	0.20	0.14
-16	0.42	0.33	0.16
-14	0.56	0.47	0.19
-12	0.78	0.70	0.23
-10	0.90	0.88	0.40
-8	0.95	0.94	0.67
-6	0.97	0.96	0.87
-4	0.98	0.98	0.97
-2	0.99	0.99	0.99
0	0.99	0.99	1.00
+2	0.99	0.99	1.00
+4	0.99	0.99	1.00

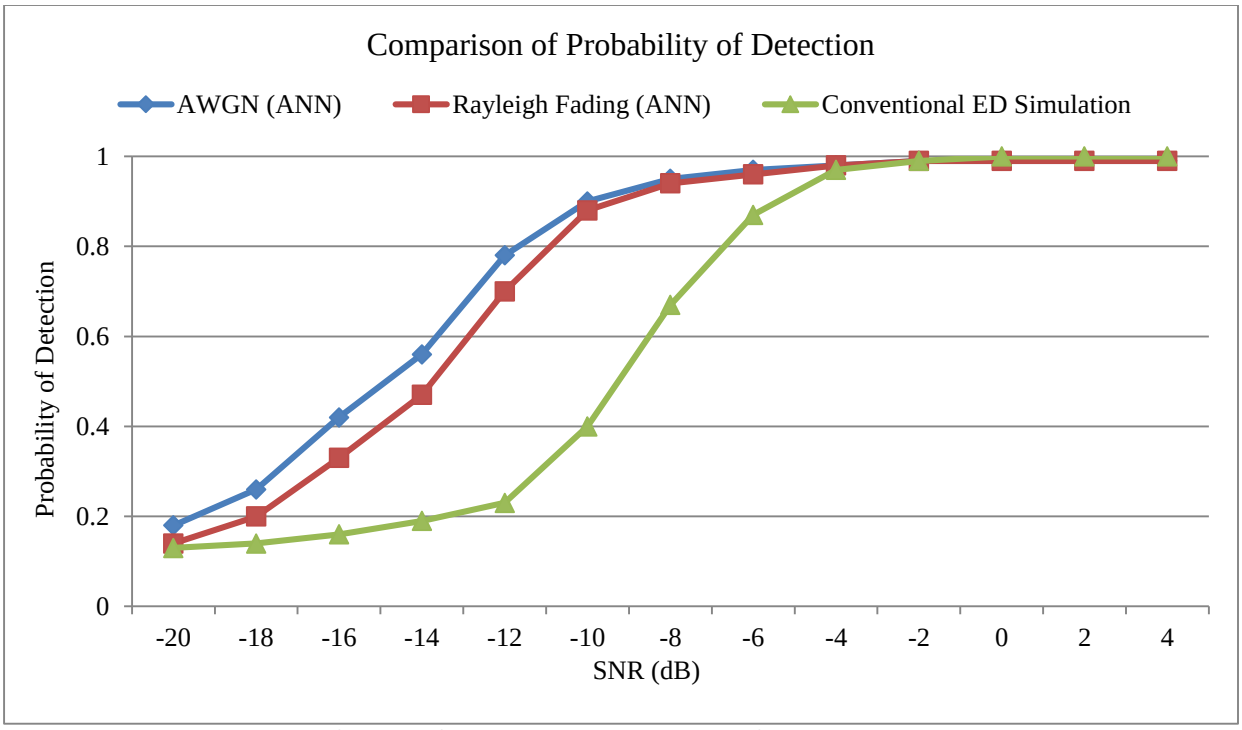

Fig. 3 Performance of ANN under AWGN and rayleigh fading vs Conventional ED

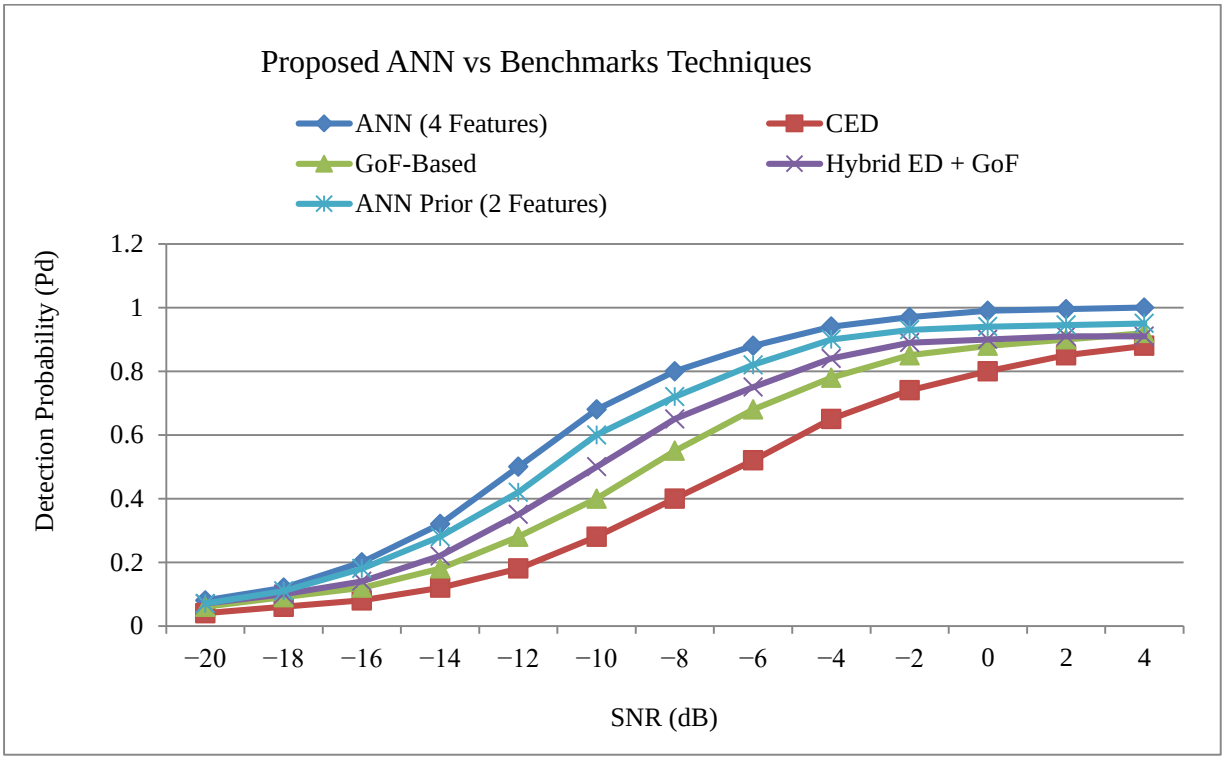

Fig. 4 Proposed ANN vs Benchmark models

The ANN approaches near-perfect detection by −6 dB, whereas energy detection requires a higher SNR to reach comparable performance. For SNR at and above 0 dB, the methods converge, but the ANN reaches high (P_d) at lower SNR and maintains greater sensitivity in adverse conditions. This behavior indicates that the ANN-based scheme is robust and well-suited for reliable spectrum sensing in cognitive radio settings.

Table 7. Comparison of P_d for ANN and benchmark techniques (N = 100)

SNR (dB)	ANN (4 Features)	CED	GoF-Based	Hybrid ED + GoF	ANN Prior (2 Features)
−20	0.08	0.04	0.06	0.07	0.07
−18	0.12	0.06	0.09	0.10	0.11
−16	0.20	0.08	0.12	0.14	0.18
−14	0.32	0.12	0.18	0.22	0.28
−12	0.50	0.18	0.28	0.35	0.42
−10	0.68	0.28	0.40	0.50	0.60
−8	0.80	0.40	0.55	0.65	0.72
−6	0.88	0.52	0.68	0.75	0.82
−4	0.94	0.65	0.78	0.84	0.90
−2	0.97	0.74	0.85	0.89	0.93
0	0.99	0.80	0.88	0.90	0.94
+2	0.995	0.85	0.90	0.91	0.945
+4	1.00	0.88	0.92	0.91	0.95

4.7. Detection Probability of ANN with Benchmark Models

Table 7 benchmarks the proposed ANN with four input features against Classical Energy Detection (CED), Goodness-of-Fit (GoF) sensing, a hybrid ED+GoF detector, and a prior ANN using two features across representative SNR levels. At very low SNR (−20 dB), the proposed model slightly outperforms all benchmarks, achieving 0.08 compared to 0.04 for CED and 0.07 for the prior ANN. The performance gap widens as SNR improves.

At −10 dB, the proposed ANN reaches 0.68, notably higher than the hybrid approach (0.50) and the two-feature ANN (0.60). By −4 dB, it achieves 0.94, maintaining a clear margin over competing methods. Near-perfect detection is attained from 0 dB onwards, whereas the benchmarks converge more slowly. These results confirm that integrating energy and statistical features enables the proposed ANN to deliver superior detection capability and robustness for spectrum sensing, as shown in Figure 4.

4.8. CFAR Detection Probability Across Sample Sizes

Table 8 presents the probability of detection versus SNR performance for a Constant False Alarm Rate (CFAR) energy detector evaluated at different sensing block sizes (N = 10, N = 100, and N = 1000). The results clearly show that as the number of samples increases, the detection performance of the energy detector improves significantly across all SNR levels. The case with N=10 has a P_d of 0.08, which increases to 0.15 for (N = 1000) at SNR -20 dB. Similarly, at −10 dB SNR, P_d improves from 0.35 (N = 10) to 0.85 (N = 1000). When the signal-to-noise ratio increases from 0 dB to +5 dB, the N has to be bigger for the detector to have a good detection, with Pd equal to 1.00 for N equal 1000. The results show that an increase in the sensing block size, N, allows better averaging, which makes it more reliable against the noise fluctuations, thus enhancing the detection probability. Figure 5 depicts the P_d trends across SNR and sample sizes.

Table 8. P_d performance of the CFAR detector across SNR and N

SNR (dB)	N = 10 Pd	N = 100 Pd	N = 1000 Pd
−20	0.08	0.10	0.15
−15	0.15	0.25	0.40
−10	0.35	0.60	0.85
−5	0.60	0.85	0.98
0	0.80	0.98	1.00
+5	0.95	1.00	1.00

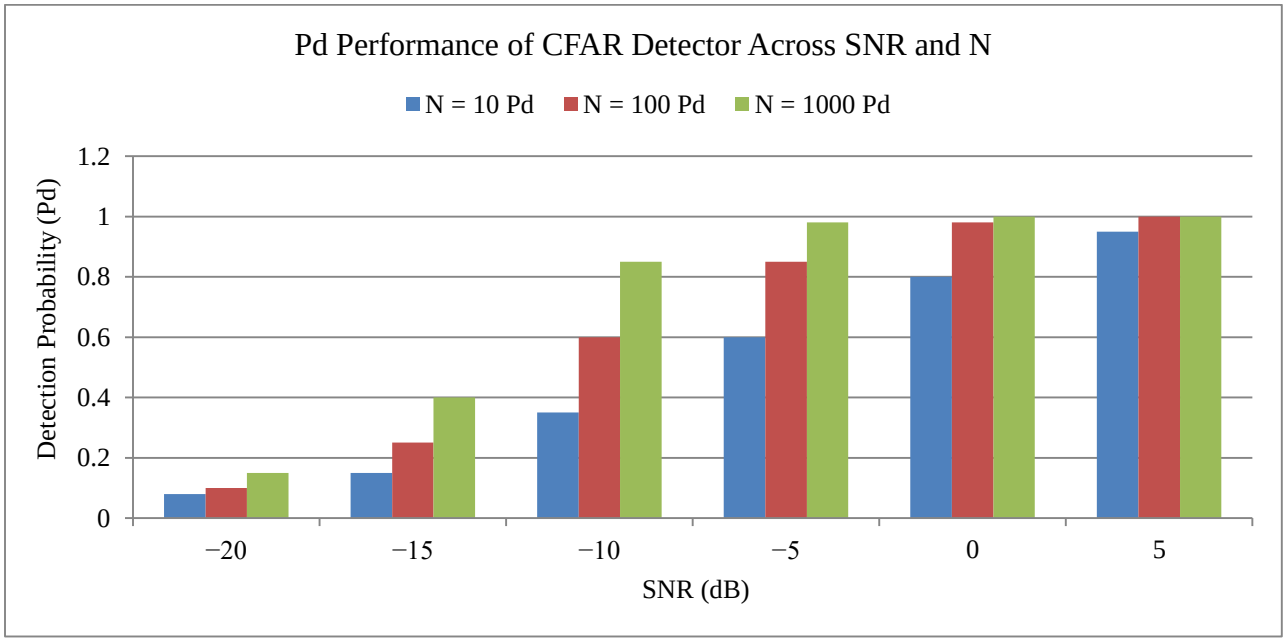

Fig. 5 CFAR detector

4.9. ROC Performance

Table 9 presents the Receiver Operating Characteristic (ROC) data, showing the P_d as a function of the P_{fa} for the CFAR energy detector with different sensing block sizes (N = 10, N = 100, and N = 1000). The results clearly demonstrate how increasing the sample size improves the detector's ability to achieve higher detection probability at the same false alarm rate. For example, at P_{fa} = 0.01, the P_d is 0.10 for N = 10, 0.50 for N = 100, and 0.98 for N = 1000. Similarly, at P_{fa} = 0.10, P_d increases from 0.35 (N = 10) to 0.85 (N = 100) and reaches 1.00 for N = 1000. At higher false alarm rates, such as P_{fa} = 0.50 and 1.00, the detector achieves very high detection probabilities across all values of N. These results highlight the trade-off between false alarm rate and detection probability and confirm that larger sensing block sizes significantly enhance the ROC performance of the CFAR energy detector. The ROC characteristics across different N values are illustrated in Figure 6.

Table 9. Receiver operator characteristics

Pfa	N=10 Pd	N=100 Pd	N=1000 Pd
0.01	0.10	0.50	0.98
0.05	0.25	0.75	0.99
0.10	0.35	0.85	1.00
0.20	0.50	0.92	1.00
0.50	0.70	0.97	1.00
1.00	1.00	1.00	1.00

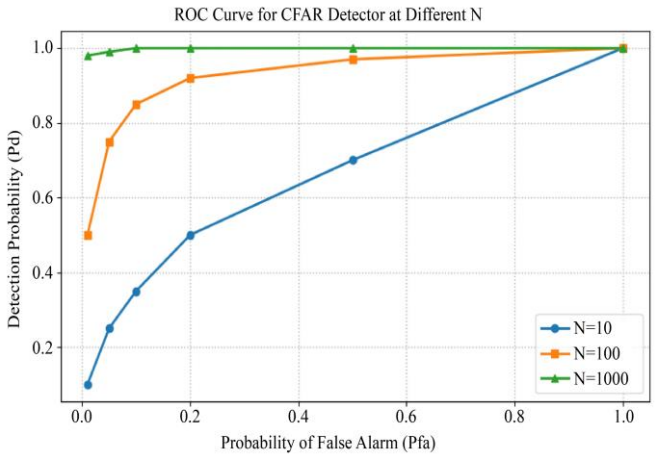

Fig. 6 ROC for CFAR detector

4.10. Performance Analysis with State-of-the-Art Models

The proposed ANN-based spectrum sensing model shows superior effectiveness compared with recent approaches. Chen et al. [25] reported a cooperative sensing framework with P_d = 91.13% at −10 dB and P_{fa} = 0.5%, while Taki et al. [26] achieved P_d = 0.86 using a chirping-based phaser method. Shalini et al. [27] developed a CNN-LSTM model reaching 92% accuracy with a 5% false alarm rate, and Wang et al. [14] obtained about 90% accuracy using a hybrid CNN-LSTM scheme. Under Rayleigh fading, the proposed ANN achieves a detection probability of 0.99 at 0 dB and 1.00 at +4 dB while maintaining a low false alarm rate. This operating point indicates strong suitability for dynamic spectrum access in cognitive radio networks.

5. Discussion

This section reports the evaluation of the proposed ANN-based spectrum sensing model across channel types, feature configurations, and baseline methods. The network uses four inputs-energy and Zhang statistics from the current and previous sensing windows—to exploit short-term temporal context and distributional cues. On the FM dataset, accuracy reached 86.82% with all four inputs, exceeding single-feature variants: energy only at 76.66%, Zhang only at 83.82%, and the current-event combination at 84.15%. In controlled studies, accuracy in AWGN rose from 86.66% (energy only) to 89.53% when energy and Zhang were combined; in Rayleigh fading, it increased from 85.53% to 88.50% for the same change in features. Detection performance improved across the SNR sweep. In AWGN, (P_d) increased from 0.18 at −20 dB to 0.99 at 0 dB. In Rayleigh fading, (P_d) progressed from 0.14 at −20 dB to 0.99 at 0 dB, narrowing the gap to AWGN at moderate and high SNR. Comparative results at −10 dB show the proposed ANN at (P_d =0.75), higher than classical energy detection (0.28), a GoF detector (0.40), a hybrid ED+GoF scheme (0.50), and a prior ANN with two inputs (0.60). At +4 dB, the proposed model reached (P_d =1.00), while the competing methods attained 0.88 (CED), 0.92 (GoF), 0.91 (Hybrid), and 0.95 (Prior ANN). Experiments with a CFAR energy detector illustrate the influence of sample Size (N). At −10 dB, (P_d) increased from 0.35 with (N=10) to 0.85 with (N=1000). Consistent behavior is observed in ROC analysis: at (P_{fa}=0.01), (P_d) rose from 0.10 ((N=10)) to 0.98 ((N=1000)). Taken together, these outcomes indicate that the proposed ANN improves accuracy and detection probability across operating regimes and maintains reliability in both AWGN and Rayleigh channels, supporting its use for dynamic spectrum access in cognitive radio networks.

Although the ANN-based spectrum sensing model attains strong accuracy under the tested conditions, several constraints remain. Training demands considerable computation and long runtimes, which limit direct use on low-power or embedded platforms. The approach also depends on labeled data, and such annotations are not always available at scale in practice. In addition, the current study evaluates performance only in AWGN and Rayleigh channels and does not capture richer, time-varying propagation effects. Future work will target shorter training cycles by introducing discriminative features that promote faster convergence and by refining the learning schedule. To reduce reliance on labels, unsupervised and semi-supervised strategies will be examined

to leverage unlabeled spectra. Lightweight and compressed network variants will also be developed for deployment on resource-constrained devices, and the evaluation will be extended to more diverse and realistic channel models through hardware-in-the-loop experiments.

6. Conclusion

This study presented an ANN-based spectrum sensing model to improve detection accuracy and robustness in cognitive radio networks under Rayleigh fading. By combining energy and Zhang statistic features from current and previous sensing windows, the model achieved 86.8% accuracy with P_d = 0.75 at −10 dB, surpassing conventional energy detection. It further reached P_d = 1.00 at +4 dB and maintained accuracies of 89.5% in AWGN and 88.5% in Rayleigh channels.

While effective, the approach relies on supervised learning and involves a high training cost, which may limit real-time deployment. Future work will explore additional features and lightweight architectures to enhance efficiency and scalability.

References

[1] P. Ramakrishnan et al., "Enhancing Spectrum Sensing in Cognitive Radio Networks using Deep Learning Models: A Solution for Low-SNR Challenges," *2024 3rd International Conference on Automation, Computing and Renewable Systems (ICACRS)*, Pudukkottai, India, pp. 1691-1696, 2024. [CrossRef] [Google Scholar] [Publisher Link]

[2] Anyi Wang, Tao Zhu, and Qifeng Meng, "Spectrum Sensing Method based on STFT-RADN in Cognitive Radio Networks," *Sensors*, vol. 24, no. 17, pp. 1-15, 2024. [CrossRef] [Google Scholar] [Publisher Link]

[3] R.G. Yelalwar, and Y. Ravinder, "Artificial Neural Network Based Approach for Spectrum Sensing in Cognitive Radio," *2018 International Conference on Wireless Communications, Signal Processing and Networking (WiSPNET)*, Chennai, India, pp. 1-5, 2018. [CrossRef] [Google Scholar] [Publisher Link]

[4] M. Suba, and D. Susan, "Performance Analysis of Cyclostationary Spectrum Sensing with Dynamic Thresholding using Artificial Neural Network Under Varying Signal-to-Noise Ratio and Noise Variance Conditions," *Journal of Intelligent & Fuzzy Systems: Applications in Engineering and Technology*, vol. 45, no. 2, pp. 3247-3257, 2023. [CrossRef] [Google Scholar] [Publisher Link]

[5] Mehmet Ali Aygül, Hakan Ali Çırpan, and Hüseyin Arslan, "Machine Learning-Based Spectrum Occupancy Prediction: A Comprehensive Survey," *Frontiers in Communications and Networks*, vol. 6, pp. 1-21, 2025. [CrossRef] [Google Scholar] [Publisher Link]

[6] Okwong Atte Enyenihi, "Towards Contention Resolution Model to Enhance Rate of Interference During Dynamic Spectrum Utilization in Cognitive Radio Network Environment," *International Journal of Science and Research Archive*, vol. 14, no. 1, pp. 1019-1028, 2025. [CrossRef] [Google Scholar] [Publisher Link]

[7] Md. Tofail Ahmed et al., "Machine Learning Approach to Energy Detection based Spectrum Sensing for Cognitive Radio Networks," *IEEJ Transactions on Electrical and Electronic Engineering*, vol. 20, no. 6, pp. 910-919, 2025. [CrossRef] [Google Scholar] [Publisher Link]

[8] M.V.S. Sairam, and Raju Egala, "Energy Detector with Adaptive Optimal Threshold for Enhancing Spectrum Sensing in Cognitive Radio Network," *International Journal of Latest Technology in Engineering Management & Applied Science*, vol. 13, no. 12, pp. 214-221, 2025. [CrossRef] [Google Scholar] [Publisher Link]

[9] P. Chandra Sekar et al., "A Support Vector Machine with Elastic-Net Regularization and Radial-Basis-Function-Based Spectrum Sensing for Cognitive Radio Networks," *2024 First International Conference on Software, Systems and Information Technology (SSITCON)*, Tumkur, India, pp. 1-5, 2024. [CrossRef] [Google Scholar] [Publisher Link]

[10] Pavan Chaudhary, Rajesh Gupta, and H. Malathi, "Machine Learning-Based Spectrum Sensing Techniques for Optimized Spectrum Utilization in Cognitive Radio Networks," *2024 3rd International Conference for Advancement in Technology (ICONAT)*, GOA, India, pp. 1-6, 2024. [CrossRef] [Google Scholar] [Publisher Link]

[11] Srinivas Samala, Subhashree Mishra, and Sudhansu Sekhar Singh, "Machine Learning and an Eigenvalue-Based Technique to Improve Cooperative Spectrum Sensing in Generalized α-κ-μ Fading Channel," *Journal of Communications*, vol. 19, no. 5, pp. 222-228, 2024. [CrossRef] [Google Scholar] [Publisher Link]

[12] Haitham Mahmoud et al., "Cooperative Spectrum Sensing with Machine Learning approaches in Cognitive Radio Networks for IoMT Applications," *2024 IEEE International Conference on Industrial Technology (ICIT)*, Bristol, United Kingdom, vol. 1-6, 2024. [CrossRef] [Google Scholar] [Publisher Link]

[13] Rohit Kumar, "Optimization of Spectrum Sensing in Cognitive Radio Using Machine Learning Approach," *2024 2nd International Conference on Device Intelligence, Computing and Communication Technologies (DICCT)*, Dehradun, India, pp. 1-5, 2024. [CrossRef] [Google Scholar] [Publisher Link]

[14] Kai Wang et al., "A Novel Multi-User Collaborative Cognitive Radio Spectrum Sensing Model: Based on a CNN-LSTM Model," *PloS one*, vol. 20, no. 1, pp. 1-27, 2025. [CrossRef] [Google Scholar] [Publisher Link]

[15] Sara E. Abdelbaset et al., "Deep Learning-Based Spectrum Sensing for Cognitive Radio Applications," *Sensors*, vol. 24, no. 24, pp. 1-22, 2024. [CrossRef] [Google Scholar] [Publisher Link]

[16] Luca Rugini, and Paolo Banelli, "Performance Analysis of Centralized Cooperative Schemes for Compressed Sensing," *Sensors*, vol. 24, no. 2, pp. 1-27, 2024. [CrossRef] [Google Scholar] [Publisher Link]

[17] Muhammad Ibkar Azki Himmawan, Dyonisius Dony Arianananda, and Sigit Basuki Wibowo, "SVM Algorithm for Cooperative Spectrum Sensing in Wireless Fading Channels," *2023 3rd International Conference on Smart Cities, Automation & Intelligent Computing Systems (ICON-SONICS)*, Bali, Indonesia, pp. 114-119, 2023. [CrossRef] [Google Scholar] [Publisher Link]

[18] Budi Bayu Murti, Risanuri Hidayat, and Sigit Basuki Wibowo, "Spectrum Sensing using SVM-based Energy Detection in Cognitive Radio Systems," *2023 6th International Seminar on Research of Information Technology and Intelligent Systems (ISRITI)*, Batam, Indonesia, pp. 101-104, 2023. [CrossRef] [Google Scholar] [Publisher Link]

[19] Pallam Venkatapathi et al., "Cooperative Spectrum Sensing Performance Assessment using Machine Learning in Cognitive Radio Sensor Networks," *Engineering, Technology & Applied Science Research*, vol. 14, no. 1, pp. 1-5, 2024. [CrossRef] [Google Scholar] [Publisher Link]

[20] Srinu Sesham, Nalina Suresh, and Abisai Fillipus Mateus Shilomboleni, "Physics-Informed Neural Networks for Sensing Radio Spectrum for Next-Generation Wireless Networks," *International Journal of Recent Technology and Engineering*, vol. 14, no. 3, pp. 1-6, 2025. [CrossRef] [Publisher Link]

[21] Lina María Yara Cifuentes, Ernesto Cadena Muñoz, and Rafael Cubillos Sánchez, "Development of a Model for Detecting Spectrum Sensing Data Falsification Attack in Mobile Cognitive Radio Networks Integrating Artificial Intelligence Techniques," *Algorithms*, vol. 18, no. 10, pp. 1-21, 2025. [CrossRef] [Google Scholar] [Publisher Link]

[22] Amit Kumar Gupta et al., "Optimizing Network Longevity and Attack Mitigation Through Adaptive Spectrum Sensing in Cognitive Radio Sensor Networks," *Research Square Preprint*, pp. 1-14, 2025. [CrossRef] [Google Scholar] [Publisher Link]

[23] Nitin B. Dhaigude, and R. A. Patil, "Hybrid Optimization-Based Channel Allocation and Scheduling in Cognitive Radio Network with CoMP JT," *International Journal of Communication Systems*, vol. 38, no. 16, 2025. [CrossRef] [Google Scholar] [Publisher Link]

[24] Obiajulu C. Emmanuel, Isa M. Danjuma, and Aliyu Sabo, "Implementation of Monte Carlo and ANFIS Techniques for Detection Threshold Estimation in Cognitive Radio," *World Journal of Advanced Research and Reviews*, vol. 27, no. 3, pp. 491-511, 2025. [CrossRef] [Google Scholar] [Publisher Link]

[25] Wangjie Chen et al., "An Integrated and Miniaturized Multi-Channel Distributed Cooperative Spectrum Sensing Technology Based on Zynq," *SAE Technical Paper Series*, 2024. [CrossRef] [Google Scholar] [Publisher Link]

[26] Haidar Taki, Didier Tanguy, and Ali Mansour, "A Simple Chirping-Based Spectrum Sensing Scheme For Cognitive Radio Applications," *International Journal of Communication Systems*, vol. 38, no. 2, 2025. [CrossRef] [Google Scholar] [Publisher Link]

[27] Shalini S. Associate et al., "Enhancing Cognitive Radio Networks for Education Systems: A Machine Learning Approach to Optimized Spectrum Sensing in Remote Learning Environments," *Journal of Infrastructure Policy and Development*, vol. 9, no. 1, pp. 1-11, 2025. [CrossRef] [Publisher Link]